Competition between spontaneous scattering and stimulated scattering in an injection-seeded Raman amplifier

J. G. Wessel, K. S. Repasky, and J. L. Carlsten
Department of Physics, Montana State University, Bozeman, Montana 59717
(Received 20 September 1995)

The amplification of a visible laser-diode beam in a gain-guided, multipass Raman amplifier is studied as a function of laser-diode and pump-laser powers. At a relatively high laser-diode power (178 nW) the amplified output grows as a simple exponential from very low gains to amplifier saturation. At a relatively low laser-diode power (2.3 nW) the behavior is more complicated, since the seeded growth and the growth from spontaneous scattering are comparable in power. The experiments, which also include an experiment with no injected laser-diode light, are modeled by a nonorthogonal-mode theory that accounts for the three-dimensional nature of the amplification process. The theory and data are found to be in close agreement in all experimental regimes studied, except at low gains with low input seed power.

PACS number(s): 42.50.Lc, 42.60.Da, 42.65.Dr

I. INTRODUCTION

Externally injected input signals are used to control or modify the output fields of many types of laser amplifiers and oscillators [1–5]. In Raman amplifiers external seeding has been shown to reduce the pumping threshold, increase the conversion efficiency, and increase the spatial quality of the output Stokes field [4–6]. Seeding of Raman amplifiers serves to stabilize the Stokes output since spontaneous scattering initiated Stokes fields have large fluctuations in frequency [7], energy [8], beam pointing direction [9], and spatial characteristics [10]. External seeding has become cheaper and simpler with the rapid expansion of the laser-diode industry, making available laser diodes with wavelengths covering much of the spectrum from long visible wavelengths to midinfrared wavelengths. These laser diodes can also be configured in external cavities, which allows the wavelength to be tuned by a significant amount in a controlled, repeatable manner.

In this paper we study, experimentally and theoretically, the amplification of a continuous-wave laser diode in a H_2 Raman amplifier and also the growth initiated by spontaneous scattering in a H_2 Raman generator. Previously we reported [5] that for moderately high energy pump-laser pulses (90–150 μJ) and a 30 nW visible laser-diode input, the output of an amplifier utilizing vibrational Raman scattering grew as an exponential of the pump power with near 100% coupling efficiency of the laser-diode input. Uchida, Nagasaka, and Tashiro [4] reported similar results from a rotational Raman scattering experiment in which an infrared laser diode was used to seed to the Stokes growth. The data was well described by a relatively simple single-mode theory of stimulated Raman scattering. In this paper, the growth of an input diode beam is studied as a function of input diode power over a wide range of amplifier gains (pump-laser energies), from very low gain to amplifier saturation. It is found that the amplifier output does not grow as an exponential in all regimes, contrary to the predictions of steady-state, single-mode theories of Raman scattering [5,11]. Instead, a theory that fully accommodates the three-dimensional nature of the amplification process, including diffraction, is needed to describe the results. This theory, which utilizes a nonorthogonal-mode expansion, has already been successfully used to model Raman generator experiments in a multipass cell [12].

Lögl, Scherm, and Maier [13] have also used the nonorthogonal-mode theory to describe single-pass Raman generator experiments. Their findings indicate that the nonorthogonal theory works well for the high gain regime but seems to breakdown at low gains. They attribute the breakdown of the theory at low gains to the use of paraxial approximations that are valid for the collimated beams inherent in stimulated scattering but do not hold for spontaneous scattering where the Stokes light scatters in all directions. They also thought the theory may break down at low gains because the nonorthogonal mode theory predicts that the output Stokes power depends on pumping geometry, whereas the standard theory of spontaneous Raman scattering, which Lögl, Scherm, and Maier found to be in agreement with their experimental results at low gains, depends on the total pumped volume but is not sensitive to the shape of the pumped region.

In this paper experimental results from both Raman amplifier experiments and Raman generator experiments done in a multipass cell are presented and compared to the predictions of the nonorthogonal-mode theory. For the amplifier, the Stokes output energy is measured as a function of input laser-diode power and pump-laser energy. For the generator, however, we measure the output Stokes energy as a function of pump energy and diameter of the exit aperture on the Raman cell. In deference to the findings of Lögl, Scherm, and Maier we also discuss the subtleties of using the nonorthogonal-mode theory at low gain. The theory and experiments, with and without an input Stokes seed, make it possible to study the interplay between spontaneous scattering and the injected seed.

In the following section a summary of the nonorthogonal-mode theory, which describes growth in a gain guided amplifier, is given. The theory is sufficiently general to describe other types of gain guided amplifiers, not just Raman amplifiers. The experimental apparatus used in our experiments is

described in Sec. III. The experimental data will be discussed and compared to the nonorthogonal-mode theory in Sec. IV. A summary and closing comments are presented in Sec. V.

II. THEORY

The theoretical model used to describe the experiment must account for growth from spontaneous scattering as well as amplification of an input seed. Previous experiments have shown [12,13] that a theory that incorporates a nonorthogonal-mode expansion of the electric field adequately describes growth initiated by spontaneous scattering. This theory readily accommodates an input seed into the amplifier, and therefore will be used to model the experiments described in this paper. The nonorthogonal-mode theory, which utilizes earlier work by Perry, Rabinowitz, and Newstein [14], has already been presented in detail elsewhere [12]. Therefore only a brief outline of the theory is presented here.

The starting point for describing growth in an amplifier is Maxwell's wave equation. In the steady state, paraxial limit the wave equation for a slowly varying electric field traveling in the positive z direction can be written as

$$[\nabla_T^2 - 2ik\partial_z + ikg(z,\boldsymbol{r}_T)]\hat{E}^{(-)}(z,\boldsymbol{r}_T) = -k^2 4\pi \hat{P}^{\dagger}_{\rm sp}(z,\boldsymbol{r}_T), \tag{1}$$

where $\nabla_T^2 = \nabla_x^2 + \nabla_y^2$, $g(z,\boldsymbol{r}_T)$ represents the gain profile, and $k = 2\pi/\lambda$ is the Stokes wave vector. The quantum operator, $\hat{P}^{\dagger}_{\rm sp}(z,\boldsymbol{r}_T)$, represents quantum fluctuations in the polarization of the medium and is included to account for spontaneous scattering. The gain profile, which in this experiment is due to a pump laser, is a focused Gaussian, i.e.,

$$g(z,\boldsymbol{r}_T) = g(z,r) = \frac{4G}{k_g \omega_g^2(z)} \exp[-2r^2/\omega_g^2(z)], \tag{2}$$

where $\omega_g(z) = \omega_g(0)[1 + z^2/z_0^2]^{1/2}$ is the radius of the pump beam, z_0 is the Rayleigh range of the pump beam, k_g is the pump-field wave vector, and G is proportional to the plane-wave gain coefficient [15]. By modeling the gain profile as a focused Gaussian, diffraction of the pump field is included *a priori*. Diffraction of the Stokes field, however, is accounted for by the transverse Laplacian.

It is convenient to write the Stokes field as the expansion

$$\hat{E}^{(-)}(z,\boldsymbol{r}_T) = \left(\frac{2\pi \Delta\nu \hbar\omega}{c}\right)^{1/2} \sum_{n,l} \hat{a}_n^{l\dagger}(z) \Phi_n^l(z,\boldsymbol{r}_T), \tag{3}$$

where $\Delta\nu$ is the amplifier bandwidth, $\hbar\omega$ is the energy of a Stokes photon, c is the speed of light, the $\{\hat{a}_n^{l\dagger}(z)\}$ are generalized photon creation operators [16], and the $\{\Phi_n^l(z,\boldsymbol{r}_T)\}$ are the nonorthogonal modes. Solving the wave equation, Eq. (1), by this ansatz has proven to be fruitful for several types of gain-guided systems ranging from diode lasers [17] to x-ray-laser amplifiers [18,19]. The modes are not arbitrary; rather, they are required to satisfy the non-Hermitian eigenvalue equation

$$[\nabla_T^2 - 2ik\partial_z + ikg(z,\boldsymbol{r}_T)] = \lambda_n^l \frac{4ik}{k_g \omega_g^2(z)} \Phi_n^l(z,\boldsymbol{r}_T), \tag{4}$$

where λ_n^l is an eigenvalue that gives the growth rate for the mode $\Phi_n^l(z,\boldsymbol{r}_T)$. As a consequence of the non-Hermiticity of Eq. (4) the modes are not orthogonal to each other, i.e.,

$$\int d^2 r_T \Phi_m^{l*}(z,\boldsymbol{r}_T)\Phi_n^j(z,\boldsymbol{r}_T) = \delta_{lj} B_{n,m}^l \neq 1, \tag{5}$$

where $(B_{n,n}^l)^2$ is referred to as the excess spontaneous-emission factor [17]. However, there is another set of modes, called the adjoint modes and denoted by $\{\Psi_n^l(z,\boldsymbol{r}_T)\}$, to which the modes $\{\Phi_n^l(z,\boldsymbol{r}_T)\}$ are orthogonal. This biorthogonality relationship is given by

$$\int d^2 r_T \Psi_m^{l*}(z,\boldsymbol{r}_T)\Phi_n^l(z,\boldsymbol{r}_T) = \delta_{m,n}. \tag{6}$$

Physically, the adjoint modes correspond to the nonorthogonal modes propagating backward through the amplifier.

In the complete theoretical solution to Eq. (1), the nonorthogonal modes themselves are written as a linear combination of Gauss-Laguerre or free-space modes [12,14]. The free-space modes, $\{U_n^l(z,\boldsymbol{r}_T)\}$, are solutions to the (Hermitian) free-space wave equation

$$(\nabla_T^2 - 2ik\partial_z) U_n^l(z,\boldsymbol{r}_T) = 0 \tag{7}$$

and as such form a complete, orthonormal set. These modes are commonly used in optics with the lowest-order free-space mode being the usual focused Gaussian. In the limit of no gain ($G \to 0$) the nonorthogonal modes become the free-space modes, to within a phase. Thus at low gains the nonorthogonal modes are approximately complete and orthogonal.

Total power in the Stokes field at a location z is obtained by integrating the intensity operator over transverse coordinates. The result is

$$\begin{aligned} P(z) &= \frac{c}{2\pi}\int d^2 r_T \langle \hat{E}^{(-)}(z,\boldsymbol{r}_T)\hat{E}^{(+)}(z,\boldsymbol{r}_T)\rangle \\ &= \Delta\nu\hbar\omega \sum_{n,p,k,l} \langle \hat{a}_n^{k\dagger}(z)\hat{a}_p^l(z)\rangle \int d^2 r_T \Phi_n^k(z,\boldsymbol{r}_T)\Phi_p^{l*}(z,\boldsymbol{r}_T) \\ &= \Delta\nu\hbar\omega \sum_{n,p,l} B_{p,n}^l (B_{p,n}^l \{\exp[(\lambda_n^l + \lambda_p^{l*})(\theta - \theta_i)] - 1\} \\ &\quad + \langle \hat{a}_n^{l\dagger}(\theta_i)\hat{a}_p^l(\theta_i)\rangle \exp[(\lambda_n^l + \lambda_p^{l*})(\theta - \theta_i)]), \end{aligned} \tag{8}$$

where the many calculations necessary to transform the left-hand side into the right-hand side (rhs) above are found in Ref. [12]. In Eq. (8) the transformation $z \to \theta = \arctan(z/z_0)$, which conveniently accounts for the focusing of the beams, has been made, θ_i locates the amplifier entrance, and the correlation $\langle \hat{a}_n^{l\dagger}(\theta_i)\hat{a}_p^l(\theta_i)\rangle$ gives the Stokes input into the amplifier. The $\hat{a}_n^{l\dagger}(\theta_i)$ are obtained by projecting the input Stokes field, $\hat{E}^{(-)}(\theta_i,\boldsymbol{r}_T)$, onto the basis of nonorthogonal modes. The result is

$$\hat{a}_n^{l\dagger}(\theta_i) = \left(\frac{c}{2\pi\Delta\nu\hbar\omega}\right)^{1/2} \int d^2 r_T \Psi_n^{l*}(\theta_i \boldsymbol{r}_T)\hat{E}^{(-)}(\theta_i,\boldsymbol{r}_T). \tag{9}$$

The output power given by the rhs of Eq. (8) has two distinct contributions. The first is the amplified spontaneous scattering, while the second is the amplified input.

Equation (8) appears to be quite complicated and indeed must be evaluated numerically for all but the simplest cases. However, for some experimentally important cases it simplifies considerably. It has been demonstrated [12] that only one term ($l=n=p=0$) is necessary to describe the growth initiated by spontaneous scattering at high gains in a Raman amplifier, whereas many Gauss-Laguerre free-space modes would be needed to do the same. For this reason the nonorthogonal modes can be considered the natural modes of the amplifier. Also under certain, rather common, experimental conditions only a few terms in Eq. (8) are needed to model the amplification of an input Stokes beam.

The final expression in Eq. (8) was obtained by assuming infinite limits on the transverse integrals and therefore represents the total Stokes power. To describe our Raman generator experiments at low gains, however, it is necessary to derive an expression for Stokes power in a finite transverse plane. We start with the first term on the rhs of Eq. (8) but this time explicitly limit the transverse integration to an aperture, i.e.,

$$P(\theta)=\Delta\nu\hbar\omega\sum_{n,p,k,l}\langle\hat{a}_n^{k\dagger}(\theta)\hat{a}_p^{l}(\theta)\rangle\int_{\text{aperture}}d^2r_T\Phi_n^k(\theta,\mathbf{r}_T)\times\Phi_p^{l*}(\theta,\mathbf{r}_T). \tag{10}$$

At low gains the nonorthogonal modes become the free-space modes, to within a phase, and as such are approximately orthogonal. Therefore the creation operators for photons in different modes are no longer correlated and the correlation function can be expressed, assuming no external Stokes input, as

$$\langle\hat{a}_n^{k\dagger}(\theta)\hat{a}_p^{l}(\theta)\rangle=\{\exp[(\lambda_n^l+\lambda_p^{l*})(\theta-\theta_i)]-1\}\delta_{n,p}\delta_{k,l}. \tag{11}$$

Substituting these approximations into Eq. (10) gives the spontaneous scattering initiated Stokes power passing through an aperture:

$$P(\theta)=\Delta\nu\hbar\omega\sum_{n,l}\{\exp[2\,\mathrm{Re}(\lambda_n^l)(\theta-\theta_i)]-1\}\times\int_{\text{aperture}}d^2r_T|U_n^l(\theta,r_T)|^2. \tag{12}$$

As will be discussed in the next section, the detectors used to monitor our experiments measure the energy per pump-laser pulse and Stokes pulse. Therefore to compare experiment to theory, Eqs. (8) and (12) are integrated over time. All calculations, including the temporal integration, are done numerically on a personal computer.

Given the input Stokes field and the gain due to the pumping field, Eqs. (8)–(12) can be used to calculate the Stokes output from a Raman generator or amplifier. Before comparing our experimental results to the theory, however, we discuss the experimental apparatus used to collect the data.

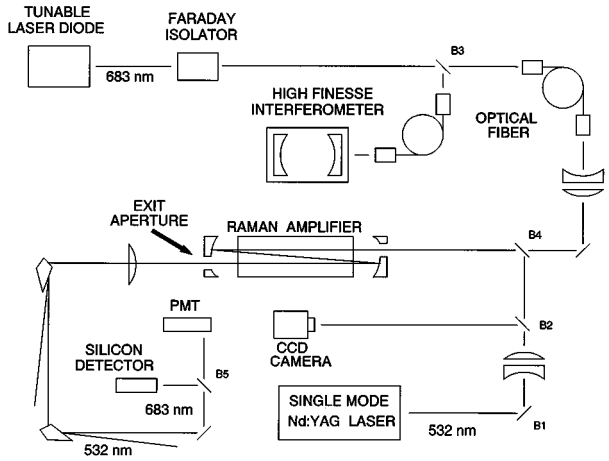

FIG. 1. Experimental apparatus used to study growth of a laser-diode seeded Stokes beam in a multiple-pass Raman amplifier pumped by a pulsed Nd:YAG laser.

III. EXPERIMENT

The experimental apparatus used in our Raman amplification experiments is shown in Fig. 1. The frequency-doubled output at 532 nm of a pulsed, single-mode, injection-seeded neodymium-doped yttrium aluminum garnet (Nd:YAG) laser was used to pump the Raman amplifier. The temporal profile of the pump beam was near Gaussian with a measured half width at half maximum (HWHM) of 3.5 ns. The spatial profile of the pump laser was also near Gaussian.

The Nd:YAG pump beam impinges on a beam splitter $B1$, shown in Fig. 1. Part of the pump beam is sent to a Laser Precision model RJP-735 pyroelectric energy detector (not shown) to monitor the input pump energy into the Raman amplifier. The rest of the beam is sent through a two-lens system for the purpose of mode matching the pump beam to the multipass cell. A beam splitter $B2$ directs part of the pump beam onto a charge-coupled device (CCD) camera. The CCD camera was used to monitor the pointing fluctuations of the pump beam. The pixel cell size of the CCD camera, which sets the resolution of the pointing fluctuation measurements, was $11\times13\ \mu\mathrm{m}^2$.

A New-Focus model 6100 continuous-wave, tunable laser diode with a center frequency of 683 nm and an output power of approximately 15 mW provided the Stokes input into the amplifier. In addition to a mechanical tuning range of approximately $\pm3\,200$ GHz, the laser diode has a tuning range of approximately 60 GHz over an externally applied voltage ramp of -3 to $+3$ V. The laser diode is isolated from the rest of the experiment by a Faraday isolator, thereby increasing the frequency and output power stability of the laser diode. Part of the beam is directed into an optical fiber by the beamsplitter $B3$. The light coming out of this optical fiber is then mode matched into a high finesse interferometer [20], which is used to monitor the relative frequency of the laser diode. The high finesse interferometer has a free spectral range of 23 600 MHz and a measured finesse of approximately 30 000, giving a resolution of greater than 1 MHz. It has a measured frequency drift of less than 7 MHz/Hr. After the beamsplitter $B3$ the laser-diode beam is coupled into a single-mode optical fiber that serves as a spatial filter. Upon exiting the optical fiber it passes through a two-lens system

that mode matches the seed beam into the multipass cell. The pump and laser-diode beams are combined at the beam combiner $B4$, shown in Fig. 1.

The multipass cell design was the same as used in previous investigations [5,12] with the following changes: The mirror spacing was 190 cm, the mode matching confocal parameter was 43.6 cm, and the number of passes was 11. Each of the mirrors has a hole in it to allow the beams to enter and exit the multipass cell. The size of the output hole, or exit aperture, was varied in the experiments. The Raman amplifier for this experiment consisted of a cell with antireflection coated windows filled with H_2 to a pressure of 34 atm. The transmission after 11 passes was measured to be approximately 74% for the pump wavelength and 66% at the Stokes wavelength.

After exiting the multipass cell, the beams were focused by a lens to ensure that all the Stokes light arrived at the detectors. The pump and Stokes beams were separated using consecutive Pelin-Broca prisms located approximately 2 m apart. Beamsplitter $B5$ directed part of the Stokes beam onto a silicon energy detector (Laser Precision RJP-765), while the remainder of the beam was incident on a Hamamatsu R928 photomultiplier tube (PMT). The output of the PMT was connected to a transient digitizer. The digitized output was then transferred to a personal computer via a general purpose interface bus. Since only the total energy of a Stokes pulse is desired, the digitizer output was integrated over time by the computer. This integrated output of the PMT was calibrated against the absolute energy readings of the silicon detector with the aid of calibrated neutral density filters. Narrowband filters (not shown in Fig. 1) that have a passband centered at the Stokes wavelength (± 5 nm) were placed in front of both the silicon detector and PMT to attenuate any scattered pump light or room light that may affect the reading.

The data was collected in the following manner: The laser-diode frequency was slowly scanned across the full Raman gain profile via a voltage output from the computer. A slow frequency drift made it difficult to hold the laser-diode frequency exactly at Raman resonance and necessitated repetitive scans of its frequency over the gain profile while the experiment was in progress. The laser-diode frequency, input pump energy, output Stokes energy from the silicon detector and from the PMT-digitizer combination, and the location of the centroid of the pump beam were monitored for each laser shot.

IV. RESULTS

The results from experiments with no input Stokes will be considered first. The growth of the Stokes beam in a Raman generator is shown as $+$'s and x's in Fig. 2. The two data were collected under identical experimental conditions except that the multipass cell exit aperture had a 3.97 mm diameter for the $+$'s and a 5.96 mm diameter for the x's. For comparison, the Gaussian pump beam had a full width at e^{-2} intensity of 1.64 mm at the exit aperture. The lines are essentially zero parameter fits of the nonorthogonal-mode theory to the data. The only parameter that was varied was the gain coefficient but the value chosen was within the published error bars. At 34 atm pressure the published value of

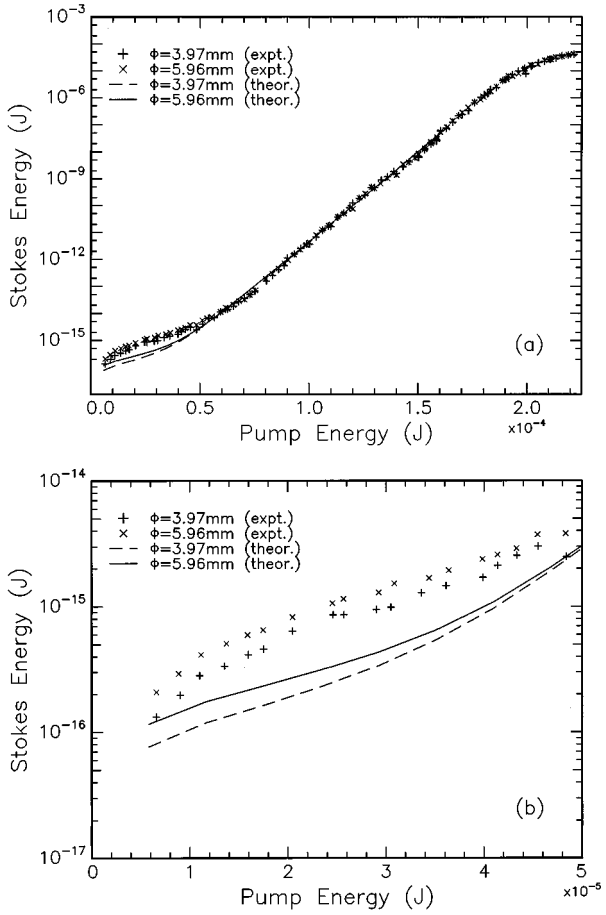

FIG. 2. Output of a Raman generator (laser-diode beam was blocked) as a function of pump-laser energy for two different exit apertures. The $+$'s ($\times$'s) correspond to an aperture with a diameter of 3.97 mm (5.96 mm). The solid lines are the predictions of the nonorthogonal theory. The data indicate that, at low pump energies, the output Stokes beam is spatially broad and is partially clipped by the small aperture. (a) Stokes growth for a wide range of pump energies. (b) An expanded view that shows that the Stokes energy depends on exit aperture at low pump energies.

the plane-wave gain coefficient, α, is $\alpha=(2.5\pm0.4)\times10^{-9}$ cm/W [15,21]. The lines were generated using $\alpha=2.1\times10^{-9}$ cm/W. However, as pointed out by Lögl, Scherm, and Maier [13], the gain parameter α represents the gain of the dominant $Q(1)$ Raman vibrational transition, whereas the PMT, even with the narrow-band filer, detects the sum of the $Q(0)$ to $Q(4)$ transitions. At high gains this distinction is unimportant; however, at low pump powers the other transitions cannot be neglected. The ratio of the total spontaneous Stokes energy to that of the $Q(1)$ transition is 1.5. This factor has been included in the nonorthogonal-mode theory at low pump energies.

In Fig. 2, Eq. (8) was used to calculate the Stokes energy for high pump energies (>70 μJ), while Eq. (12) was used for the lower pump energies. For reasons that will be discussed shortly it was necessary to include only one mode ($n=p=l=0$) in Eq. (8), while many modes ($0\leq n<85$ and $0\leq l<20$) were needed in Eq. (12). The theoretical lines are smooth and continuous even though different formulas were used, indicating that the approximations used in deriving Eq. (12) are justified. To account for the multiple passes used in

the experiment, we simply multiply θ by s, where s is the effective number of passes the beams make through the amplifier [22]. s is the total number of beam passages multiplied by a factor that takes into account optical losses due to incomplete reflections from the mirrors and incomplete transmissions through the cell windows. In our experiments the number of beam passages through the cell was 11, while the effective number of passes was 9.5.

For pump energies greater than approximately 70 μJ and less than 180 μJ, where the amplifier begins to saturate, the output Stokes grows as an exponential in the pump energy regardless of the aperture size. In this range of pump energies the data shows some scatter but, in general, there is no measurable difference in Stokes energy between the large aperture and the small aperture data. This type of growth is predicted by plane-wave theories [5,11] of Raman scattering as well as the nonorthogonal-mode theory. However, to predict the Stokes growth for pump energies less than 70 μJ it is necessary to employ a theory, such as the nonorthogonal-mode theory, which takes into account the three-dimensional nature of the amplification process.

At low pump energies the output Stokes energy shows a characteristic ''hump'' due to the contribution of higher-order spatial modes seeded by spontaneous scattering. Figure 2 shows that the Stokes energies measured with the small aperture installed are consistently less than those measured the large aperture in place. It is apparent that at low gains the Stokes beam is much larger than the pump beam and is partially clipped by the exit aperture. A physical picture of why the Stokes beam is so broad can be obtained by considering the following model of spontaneous scattering. Spontaneous scattering is vibrational Raman scattering in H_2 can be calculated by assuming the Raman medium is a fully inverted two level amplifier. The noise in such an amplifier is one photon per mode; that is, the spontaneous scattering initiated output behaves as if one photon per mode were input into and amplified by a noiseless amplifier [23]. Thus to model the spontaneous scattering in the amplifier it is assumed that each of the infinite number of spatial modes that couple to the pump beam and experience growth are seeded by one noise photon. The total output Stokes energy is finite, however, since the input noise photons are not measurable. A mathematical manifestation of the immeasurability of the input noise photons is the ''-1,'' which occurs in the expressions, Eqs. (8) and (12), which describe growth from spontaneous scattering.

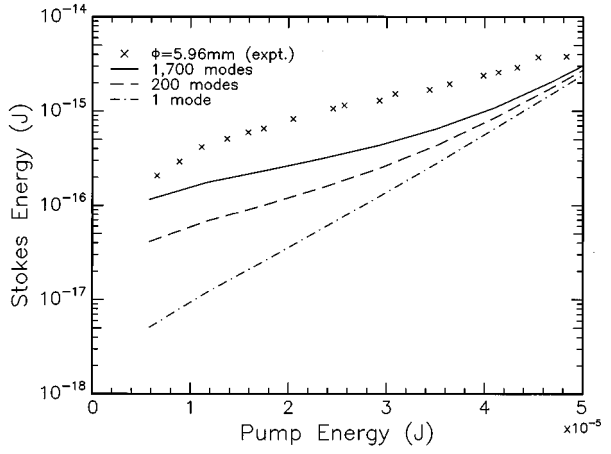

FIG. 3. Output Stokes energy as a function of the number of modes included in the nonorthogonal-mode theory. At relatively large pump energies the Stokes field grows predominantly in only one mode, while at low pump energies many modes are populated.

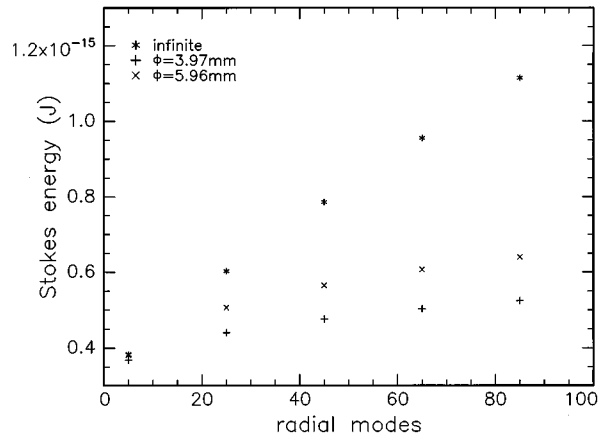

FIG. 4. Theoretical output Stokes energy as a function of the number of radial modes included in the nonorthogonal-mode theory. Data for three different apertures indicate that as the aperture size increases, so too must the number of modes included in the theory.

It is rarely necessary to consider growth in all the spatial modes, however, since only a finite number of these modes couple strongly to the pump and experience significant growth. In our experiments the pump laser is spatially Gaussian; hence, the low-order Stokes modes tend to have the largest growth rates. Also, the exit aperture utilized in the experiments partially filters out the higher order modes, further reducing the effect of higher-order modes on the output Stokes energy. At larger pump energies the Stokes grows predominantly in the lowest-order mode which is spatially narrow. The Stokes beam can even become narrower than the pump beam at high pump energies. This spatial gain narrowing is predicted by the nonorthogonal-mode theory and has been experimentally measured [13]. Since the Stokes beam is narrow at high gains the measured Stokes energy is the same for both apertures. At lower pump energies, however, the Stokes field has substantial growth in many modes. High-order modes tend to be spatially wider than low-order modes; therefore, the Stokes beam can be significantly wider than the pump beam.

Figures 3 and 4 illustrate how the number of modes included in the theory affect the theoretical Stokes output energy. First consider Fig. 3 in which the 5.96-mm aperture Stokes output energy given by Eq. (12) is computed using 1 700 modes (85 low-order radial modes and 20 low-order angular modes), 200 modes (10 low-order radial modes and 20 low-order angular modes), and the lowest-order mode. The radial modes are indexed by n, while the angular modes are indexed by l in Eq. (12). The graph shows that at low pump energies many modes contribute to the output Stokes energy. At higher pump energies, however, the difference between 1 700 modes and one mode is very small, indicating that the Stokes field grows predominantly in the lowest-order mode. Figure 4, obtained by integrating Eq. (12) at $G=0.3$ (33 μJ pump energy) as a function of the number of radial

modes, shows the effect of aperture size on output Stokes energy. All data in this figure was calculated using 20 angular modes. High-order angular modes weakly couple to the pump beam [14]; therefore, including more angular modes increases the output Stokes energy little. Notice that the Stokes energy increases nearly linearly in the number of radial modes for the infinite exit aperture. With the finite apertures, however, the Stokes energy is a slowly increasing function of the number of radial modes and appears to be converging to finite values. Limited computing power prevented us from including more modes in the calculations. The calculations indicate that the number of modes that need be included in the theory to properly describe an experiment depend on experimental parameters.

The theory and experiment shown in Fig. 2 are in close agreement except at low pump energies. Both the data and the nonorthogonal-mode theory exhibit the characteristic ''hump'' at low pump energies but it is more pronounced in the data. Interestingly, however, the ratio of theoretical Stokes energy with the large aperture in place to the theoretical Stokes energy with the small aperture installed in nearly the same as the corresponding experimental ratio. For example, at a pump energy of 20 μJ the theoretical ratio is 1.42 while the experimental ratio of large aperture output Stokes energy to small aperture output Stokes energy was 1.34. We do not have a complete explanation for the discrepancy between the theory and experimental results but propose it may be do to one or more of the following reasons. First, at low gains Stokes light scatters in all directions. Some of this light may reflect off the multipass cell mirrors and/or Raman cell walls and enter the PMT. The theory does not account for this light. We are currently modifying our experimental setup to reduce the likelihood of scattered light impinging on the Stokes detectors. Including more modes in the nonorthogonal-mode theory would increase the theoretical Stokes output energy. However, Figs. 3 and 4 imply that this effect would probably be small. Another consideration, as pointed out by Lögl, Scherm, and Maier [13] who also found

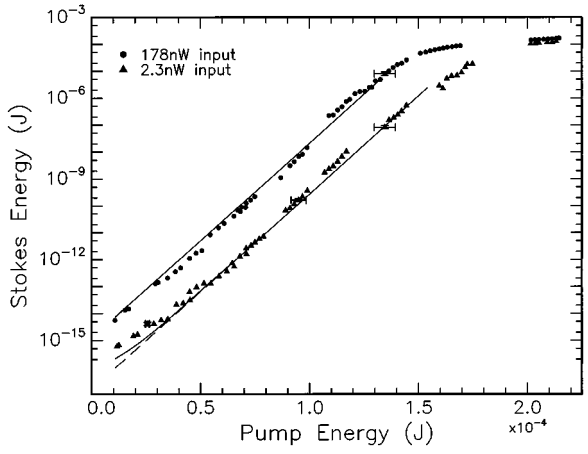

FIG. 5. Data points ●'s and ▲'s represent seeded growth for input Stokes powers of 178 and 2.3 nW, respectively. The dashed lines are the predicted growth if the amplifier were noiseless (effects of spontaneous scattering were neglected), while the solid line includes both the amplified input and amplified spontaneous scattering. The falloff in Stokes energy at large pump energies is due to amplifier saturation.

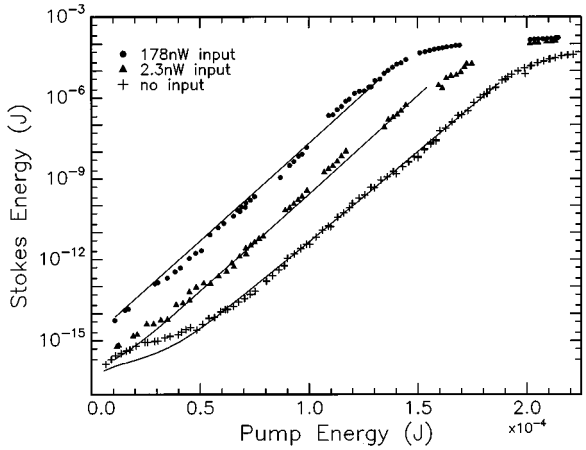

FIG. 6. Small aperture generator data from Fig. 2 is combined with the amplifier data found in Fig. 5. It is evident from the plot that to maintain a constant output signal-to-noise ratio, the input Stokes seed power must be significantly larger at low pump energies than high pump energies.

a discrepancy between theory and experiment at low gains, is that the nonorthogonal-mode theory is a paraxial theory that cannot properly describe the Stokes light that scatters in all directions at low gains. However, by collecting only the Stokes light which is on axis or nearly so, we claim it should be justifiable to use a paraxial theory to model our experiments.

We now turn our attention to the experimental data obtained when the Stokes seed was injected into the Raman medium. All experiments that utilized the Stokes seed were done with the small aperture ($\phi = 3.9$ mm) in place. The slow frequency drift of the laser diode made it difficult to hold the frequency on Raman resonance. Therefore the data was collected as the laser diode was repetitively tuned across the Raman line shape. The resulting data, Stokes energy versus relative laser-diode frequency, is similar to that shown in Fig. 2 of Ref. [5]. The measured line shapes were found to be of Gaussian shape in accord with Raman theory [11], but were found to be wider than theory. For example, at a pump energy of 140 μJ and a Stokes input power of 178 nW with the experimentally measured linewidth is (252 ± 6) MHz (HWHM), while the theoretical linewidth predicted is (131 ± 6) MHZ (HWHM). This discrepancy is larger than that seen in a previous experiment [5]; however, the error bars are smaller in the present experiment. Part of the discrepancy is due to the fact that the theory does not take into account the pump linewidth, which is approximately 30 MHz (HWHM). Including the finite linewidth of the pump broadens the predicted Stokes linewidth. The source of the remaining discrepancy is unknown at this time. It does not appear to be experimental artifact, however, since we have measured the linewidth many times, and although there is some scatter in the experimental data, the measured linewidth is, on average, nearly twice that predicted by the plane-wave, steady-state theory [11]. Later, in Figs. 5 and 6, the output Stokes energy vs pump energy for two different values of input Stokes energy is plotted. In these plots only the data points which were collected when the input Stokes frequency was at or very near exact resonance are displayed. We have implicitly assumed that the output Stokes energy is largest

when the laser diode is tuned to Raman resonance.

Figure 5 shows the output Stokes energy vs pump energy for input laser-diode powers of 178 nW (circles) and 2.3 nW (triangles). In both cases the laser-diode beam had the same confocal parameter as the pump beam and therefore was most efficiently coupled into the lowest-order nonorthogonal mode. Injecting 178 nW into the lowest-order mode makes the effect of spontaneous scattering on the output Stokes energy negligible. In this case the amplified input is much larger than the amplified spontaneous scattering in all the other modes and the amplifier output grows as an exponential for all pump energies until the amplifier saturates. Injecting only 2.3 nW into the amplifier, however, is not sufficient to dominate the amplified spontaneous scattering for all values of the pump energy. At higher pump energies, where only one spontaneously seeded mode contributes significantly to the Stokes output energy, the externally seeded lowest-order mode is dominant. However, at low pump energies many spontaneous scattering seeded modes are significant and the externally seeded mode is ''washed output'' by the amplifier noise.

The dashed lines in Fig. 5 show the amplification of the input Stokes beam as predicted by the nonorthogonal mode theory. The effects of spontaneous scattering were not included in the calculation of the dashed lines. The amplified input seed was calculated using only the lowest-order mode in the second term on the rhs of Eq. (8). The results of this calculation for the two different input seed powers are shown as dashed lines. However, even in the presence of a seed, Eq. (8) indicates that the total output Stokes power is the linear combination of the spontaneous scattering initiated Stokes field and the amplified input. The amplified spontaneous scattering was calculated as it was in Fig. 2; Eq. (12) was used for low gains, while Eq. (8) was used at high gains. The solid lines in Fig. 5 represent the total Stokes output power: amplified input and amplified spontaneous scattering. Since the amplified input and amplified spontaneous scattering add linearly and the data is plotted on a logarithmic scale, including the effects of spontaneous scattering on the 178 nW seeded data, changes the output Stokes energy negligibly. At 2.3 nW seed power, however, adding the amplified spontaneous scattering to the amplified input increases the output energy by a noticeable amount at low pump energies.

The data and theory from Fig. 2 (small aperture) and Fig. 5 are combined in Fig. 6 to facilitate a comparison of the growth from spontaneous scattering to externally seeded growth. From this plot we can estimate the amount of spontaneous scattering that is effectively seeding the amplifier by taking the ratio of externally seeded Stokes energy to the spontaneous scattering seeded Stokes at a particular pump energy. For example, at a pump energy 100 μJ taking the ratio of either 2.3 or 178 nW seeded Stokes energy to the spontaneously initiated Stokes energy yields an effective spontaneous scattering input of 0.04 nW. This means that to attain an amplifier signal-to-noise ratio of unity at 100 μJ pump energy it is necessary to inject approximately 0.04 nW seed power into the lowest-order mode. It should be pointed out that this method of estimating the amount of spontaneous scattering is inaccurate for the experimental regimes, such as the low gain regime, in which the externally seeded Stokes growth takes place in only one mode while the spontaneous scattering initiated growth occurs in many modes, each having a different growth rate.

V. CONCLUSION

We have studied experimentally and theoretically the growth of an input Stokes beam in a Raman amplifier configured in a multipass cell. Results from a Raman generator were also included. Generator data indicates that at low pump energies the Stokes beam is significantly wider than the pump beam but at higher pump energies the Stokes beam narrows. In the future we plan to directly measure the Stokes profile at very low Stokes energies using an image intensified CCD camera.

The amplifier experiments show that for relatively large input seed power (178 nW) the output of the amplifier grew as an exponential in the pump power. At lower input seed power (2.3 nW) the amplifier output was a combination of amplified input and amplified spontaneous scattering. It was also found that the external Stokes seed more easily dominates the spontaneous scattering at high gains than low gains. The data, from both the generator and amplifier experiments, were modeled with a nonorthogonal mode theory of Raman scattering, which takes into account the focused Gaussian nature of the pump and Stokes beams. The theory was in good agreement with the data except at low pump powers. Also at low gains, where noncollimated spontaneous scattering occurs, care must be exercised to ensure that the correct number of modes is used in the calculations.

ACKNOWLEDGMENTS

This work was supported by National Science Foundation Grant No. PHY-9424637. We would also like to thank M. Maier for sending us preprints of Ref. [13].

[1] D. Böhm, F. Von Moers, and A. Hese, IEEE J. Quantum Electron. **25**, 1720 (1989).

[2] P. Cassard and J. Lourtioz, IEEE J. Quantum Electron. **24**, 2321 (1988).

[3] M. D. Selker, R. S. Afzal, J. L. Dallas, and A. W. Yu, Opt. Lett. **19**, 551 (1994).

[4] M. Uchida, K. Nagasaka, and H. Tashiro, Opt. Lett. **14**, 1350 (1989).

[5] J. G. Wessel, K. S. Repasky, and J. L. Carlsten, Opt. Lett. **19**, 1430 (1994).

[6] S. Wada, H. Moriwaki, A. Nakamura, and H. Tashiro, Opt. Lett. **20**, 848 (1995).

[7] R. C. Swanson, P. R. Battle, and J. L. Carlsten, Phys. Rev. A **42**, 6774 (1990).

[8] I. A. Walmsley and M. G. Raymer, Phys. Rev. Lett. **50**, 962 (1983).

[9] S. J. Kuo, D. T. Smithey, and M. G. Raymer, Phys. Rev. A **45**, 2031 (1992).
[10] M. D. Duncan, R. Mathon, L. L. Tankersley, and J. Reintjes, J. Opt. Soc. Am. B **7**, 1336 (1990).
[11] M. G. Raymer, J. Mostowski, and J. L. Carlsten, Phys. Rev. A **19**, 2304 (1979).
[12] P. R. Battle, J. G. Wessel, and J. L. Carlsten, Phys. Rev. A **48**, 707 (1993).
[13] S. Lögl, M. Scherm, and M. Maier, Phys. Rev. A **52**, 657 (1995).
[14] B. N. Perry, P. Rabinowitz, and M. Newstein, Phys. Rev. A **27**, 1989 (1983).
[15] The relationship between G and the plane-wave gain coefficient, α, is $G=\alpha P/\lambda_g$, where P is the peak pump-laser power.
[16] I. H. Deutsch, J. C. Garrison, and E. M. Wright, J. Opt. Soc. Am. B. **8**, 1244 (1991).
[17] K. Petermann, IEEE J. Quantum Electron. **15**, 566 (1979); H. A. Haus and S. Kawakami, *ibid.* **21**, 63 (1985); W. Streifer, D. R. Scifres, and R. D. Burnham, *ibid.* **16**, 418 (1978).
[18] P. Amendt, R. A. London, and M. Strauss, Phys. Rev. A **44**, 7478 (1991).
[19] A. E. Siegman, Phys. Rev. A **39**, 1253 (1989); **39**, 1264 (1989).
[20] K. S. Repasky, L. E. Watson, and J. L. Carlsten, Appl. Opt. **34**, 2615 (1995); K. S. Repasky, J. G. Wessel, and J. L. Carlsten, Appl. Opt. (to be published).
[21] W. K. Bischel and M. J. Dyer, J. Opt. Soc. Am. B **3**, 677 (1986).
[22] D. C. MacPherson, R. C. Swanson, and J. L. Carlsten, IEEE J. Quantum Electron. **25**, 1741 (1989).
[23] Rigorously, the amount of noise is one photon per *orthogonal* mode. However, at low gains the modes $\Phi_n^l(\theta,r_T)$ are approximately orthogonal. For a discussion on noise properties of a Raman amplifier, see P. R. Battle, R. C. Swanson, and J. L. Carlsten, Phys. Rev. A **44**, 1922 (1991).